Astron. Astrophys. 341, 348–354 (1999)

ASTRONOMY AND ASTROPHYSICS

A survey of molecular gas content of galaxies at $0.08 < z < 1.06$

K.-Y. Lo[1,2,3], **H.-W. Chen**[2,4], **and P.T.P. Ho**[5]

[1] Max-Planck-Institut für Extraterrestrische Physik, Postfach 1603, D-85740 Garching, Germany
[2] Astronomy Department, University of Illinois, 1002 West Green Street, Urbana, IL 61801, USA
[3] Institute of Astronomy and Astrophysics, Academia Sinica, Taipei 115, Taiwan, ROC
[4] Department of Physics and Astronomy, State University of New York, Stony Brook, NY 11794, USA
[5] Harvard-Smithsonian Center for Astrophysics, 60 Garden Street, Cambridge, MA 02128, USA

Received 24 July 1998 / Accepted 30 September 1998

Abstract. The study of high redshift galaxies has made tremendous progress in the last few years. In order to understand their evolution, it is important to probe the gas content of distant "normal" galaxies beyond z $\sim$ 0.3. We searched for CO emission from a sample of galaxies in the redshift range of 0.35 to 1.06. Given the current limited sensitivity, we can only place upper limits to the gas content of these progenitors to luminous field galaxies of $\sim 3 \times 10^{11} \mathrm{M}_\odot$. We also searched a sample of distant luminous IR galaxies and detected two new galaxies at z $\sim$ 0.1. The upper limits to and the detection of CO emission from these distant galaxies are consistent with the suggested upper limit to galaxy masses of $10^{12} \mathrm{M}_\odot$ posed by the cooling time argument.

Key words: submillimeter – galaxies: ISM – galaxies: evolution – ISM: molecules

1. Introduction

The identification and study of high redshift galaxies are necessary for reconstructing the history of galaxy formation and evolution, which depends on the cosmological parameters such as the baryon density, and the density and nature of dark matter. In the last few years, such studies have made tremendous progress. Many deep galaxy surveys have been carried out and revealed an excess of faint blue galaxies at redshifts $0.2 < z \lesssim 1.2$ (e.g. Ellis 1997 and references therein). Various studies of damped Lyα and metal-line absorption systems observed in the spectra of background QSOs have also led to the identification of luminous galaxies that may be the precursors of current day bright galaxies (Wolfe et al. 1986; Steidel 1993; Wolfe & Prochaska 1998). Recent results from Hubble Deep Field further confirm the previous studies that the bulk of star formation started at $z < 2$ with a decreasing rate toward current epoch (Lanzetta et al. 1996; Guzmán et al. 1997). Furthermore, a broad-band photometric technique adopted by Steidel et al. (1996) has proven very effective in searching for galaxies at redshifts $z \approx 3$. They found that massive star-forming galaxies were already in place when the universe was only 15% of its current age (Steidel et al. 1998).

Send offprint requests to: K.-Y. Lo (kyl@biaa.sinica.edu.tw)

Given that stars are formed from gas, determining the gas content and physical conditions of neutral gas in galaxies at different redshifts is necessary for understanding how and why galaxies evolve. To probe the gas content of distant galaxies, it is generally easier to detect the millimeter wavelength emission from the tracer molecule, CO, than the 21 cm hyperfine transition of the ground state of atomic hydrogen. This advantage of high frequency is mainly because the flux density of thermal emission increases as ν^2. Specifically, the signal to noise ratio of a detection, $\mathrm{S/N} \propto \Omega_\mathrm{s}\ \mathrm{T_b}\ \nu^{2.5}\ \mathrm{T_s^{-1}} \sqrt{\Delta \mathrm{v}\ \tau}\ \mathrm{A_e}$, where $\Omega_\mathrm{s},\ \mathrm{T_b},\ \mathrm{T_s},\ \Delta \mathrm{v},\ \tau,\ \mathrm{A_e}$ are the solid angle and brightness temperature of the source, the system temperature, the line-width, the integration time and effective area of the telescope, respectively.

Hence, most efforts to detect neutral gas emission in high-z galaxies have concentrated in the millimeter wavelength range, but the detectability is primarily limited by available sensitivity. For example, Wiklind & Combes (1994) searched for CO emission in the direction of QSO's that show damped Lyα absorption lines with $0.5 \lesssim z \lesssim 2.8$ in their spectra, but were only able to provide upper limits of typically more than $10^{11}\ \mathrm{M}_\odot$ of $\mathrm{H_2}$.

Nevertheless, CO emission has been unambiguously detected out to $z = 4.69$ and $z = 4.41$ in two radio-quiet quasars, BR1202−0725 (Ohta et al. 1995; Omont et al. 1995) and BRI1335−0417 (Guilloteau et al. 1997), at $z \approx 2.6$ in three gravitationally lensed systems (Brown & Vanden Bout, 1992; Barvainis et al. 1994; Barvainis et al. 1998), at $z = 2.394$ in a radio galaxy 53W002 (Scoville et al. 1997), and at $z = 0.37$ from 3C48 (Scoville et al. 1993; Wink et al. 1997). CO emission from ultra-luminous infrared galaxies has been detected out to $z = 0.27$ (Solomon et al. 1997). We summarize the properties of these high redshift objects in Table 1, where $\mathrm{S}_\nu \Delta \mathrm{V}$ is the flux, $\mathrm{S}_{100\mu m}$ is the flux density observed at 100(1+z) μm and L'_{CO} is defined in Eq. (3) below.

Thus, the detection of CO emission from high-z galaxies has been predominantly from those with unusual properties, or under special circumstances such as gravitational lensing. In order to probe the gas content of "normal" galaxies, we have chosen a sample of galaxies at intermediate redshifts: $0.35 < z < 1.06$, from galaxies in the vicinity of QSOs at the same redshift as

Table 1. Properties of high-z objects (uncorrected for gravitational magnification)

source	z	CO line	$S_\nu \Delta V$ Jy km s^{-1}	$S_{100\mu m}$ Jy	$L'_{\rm CO}$ 10^{10} K km s^{-1}pc^2	$M(H_2)$ $10^{10} M_\odot$	references
3C 48	0.3695	(1→0)	2.4	< 1.02	0.9	4.2	1
PG1634+706	1.3371	(2→1)	< 0.9	...	0.5	< 2.2	2
F10214+4724*	2.2855	(3→2)	4.1	...	4.7	21.8	3
53W002	2.394	(3→2)	1.6	...	2.0	9.3	4
H1413+117*	2.5585	(3→2)	8.1	0.19	10.3	47.5	5,6
MG0414+0534	2.639	(3→2)	2.6	...	3.7	17.0	2
BRI1335−0417	4.41	(5→4)	2.8	...	3.1	14.3	7
BR1202-0725	4.69	(7→6)	3.1	0.09	1.9	8.8	8,9

1. Wink et al. 1997; 2. Barvainis et al. 1998; 3. Solomon et al. 1992; 4.Scoville et al. 1997;
5. Barvainis et al. 1994; 6. Barvainis et al. 1995; 7. Guilloteau et al. 1997; 8. Omont et al. 1996;
9. Isaak et al. 1994. * gravitationally lensed system.

the metal line absorption systems in the QSO spectra. These are almost certainly the progenitors of normal, but luminous, field galaxies (Steidel 1993).

We also included galaxies that belong to the class of luminous IR galaxies drawn from a catalog of optically faint IRAS sources (Klaas & Elsässer 1993) and three from a sample of ultra-luminous galaxies (Zhao et al, private communications).

In total, we have a sample of 23 galaxies: 8 are progenitors to "normal" field galaxies ($0.35 < z < 1.06$), 13 are IRAS galaxies ($0.1 < z < 0.59$), 1 BL Lac object (z=0.52) and 1 E+A galaxy (z=0.088).

We have adopted a Hubble constant, $H_o = 75\,{\rm km\,s^{-1}}$ Mpc^{-1}, and a decceleration factor, $q_0 = 0.5$, throughout this paper.

2. Observations and data reduction

The observations were done with the IRAM 30-m telescope at Pico Veleta in Spain, both in August of 1994 and August of 1996, and with the NRAO 12-m telescope at Kitt Peak, USA, in June of 1995 and during the following year using available unscheduled telescope time. The total telescope time used was about 7 days for the 30m and about 14 days for the 12m.

At the IRAM 30-m telescope we used the 3-, 2- and 1.3-mm receivers, depending on the redshift of the source, to search for three adjacent rotational transitions of CO. The receivers were all used in the single-side-band mode. We used both the 512-channel 1-MHz filter-bank spectrometer and the auto-correlator, with resolution ranging between 1 and 3 km s^{-1}. During data reduction, the spectra were smoothed typically to 20–30 km s^{-1}. The beam sizes (FWHM) at 3-, 2- and 1.3-mm are 24″, 18″ and 13″, respectively. The observations were made with a nutating secondary, with offsets of $\pm 4'$ in azimuth. Pointing checks were made regularly at nearby continuum sources, and the pointing is typically quite good, with rms variations of $\sim 5''$.

At the NRAO 12-m telescope, we searched for only the CO $(1-0)$ line in the 3-mm band with the 55″ beam. All observations were made with the dual polarization SIS mixer receivers, and a nutating subreflector to switch between the source and reference positions 4' away in azimuth at 1.25 Hz. We used the 256-channel 2-MHz filter-bank spectrometer.

The data consist of a series of individual spectra with a 5-minute integration time. The data from the 12 m and the 30 m telescopes were reduced using the programs UNIPOPS and CLASS, respectively. The individual spectra were baseline corrected with a first order approximation, hanning smoothed to increase the S/N ratio, and added up to form the final spectrum for each source.

3. Results and analysis

The various beam-widths used $-55''$, 24″, 18″, 13″ correspond to a linear scale of 91, 40, 30 and 22 kpc at z = 0.1, respectively. The galaxies searched may be considered unresolved by the telescope beams, and the following analysis of the measurements is made under this approximation.

The relevant observational parameters for each source are listed in Tables 2–4. The total integration time is shown in the column, T_{int}, whereas δv and $\sigma_{\rm rms}$ show the resolution and the r.m.s. noise of the final spectrum, respectively. $M({\rm H_2})$ gives the $\rm H_2$ mass. In Table 3, we also listed the observed 100μm flux densities in Jy, if available in the IRAS catalogue. For the spectra showing line emission, the spectra were fitted with a Gaussian profile to obtain the peak brightness temperature, T_{peak}, and the full width at half maximum (FWHM), Δv.

The integrated CO luminosity emitted by the source is given by

$$L_{\rm CO} = 4\pi D_L^2 S_{\nu_{obs}} \Delta\nu_{obs} = 4\pi \frac{D_L^2}{(1+z)} S_{\nu_{obs}} \Delta v \frac{\nu_0}{c}\,, \qquad (1)$$

where D_L is the luminosity distance, $\rm S_{\nu_{obs}}$ the observed flux density at $\nu_{\rm obs}$, the observed frequency, $\nu_{\rm o}$ the rest frequency, and Δv the line-width in km s^{-1}.

$$S_{\nu_{obs}} \Delta v = \Omega_s T_b(\nu_{obs}) \Delta v \frac{2k\nu_{obs}^2}{c^2} = \Omega_b I_{\rm CO} \frac{2k\nu_0^2}{(1+z)^2 c^2}, \qquad (2)$$

where $\Omega_s, \Omega_b, T_b(\nu_{obs})$ and $I_{CO} = T_{mb}\Delta v$ are the source solid angle, the telescope beam solid angle, the observed brightness

temperature and the CO integrated intensity, respectively. The second equality holds if all the emitting sources are smaller than the beam size, Ω_b, such that the main-beam temperature, T_{mb}, is the beam diluted observed brightness temperature, $T_{mb} = (\Omega_s/\Omega_b)T_b(\nu_{obs})$. Note that $T_b(\nu_{obs}) = T_b(\nu_o)/(1+z)$, where $T_b(\nu_o)$ is the instrinsic cloud brightness temperature. Therefore, in terms of the observables and the angular distance $D_A(= D_L/(1+z)^2)$,

$$L'_{\rm CO} \equiv \frac{c^3}{8\pi k\nu_0^3} L_{\rm CO} = \Omega_b I_{\rm CO} \frac{D_L^2}{(1+z)^3} = \Omega_s T_b(\nu_o) \Delta v D_A^2. \quad (3)$$

For the same source, the $L'_{\rm CO}$ of the J $\rightarrow$ J-1 transition is related to that of the 1 $\rightarrow$ 0 transition via the following:

$$\frac{L'_{\rm CO(J)}}{L'_{\rm CO(1)}} = \frac{\Omega_b(J)}{\Omega_b(1)} \frac{I_{CO(J)}}{I_{CO(1)}} = \frac{\Omega_s(J)}{\Omega_s(1)} \frac{T_b(J)}{T_b(1)}, \quad (4)$$

where J and 1 denote the quantities at the two transitions. The first equality gives the ratio in terms of observed quantities and the second relates to the source parameters. In comparing distant galaxies at different z when different CO transitions are observed, $L'_{\rm CO}$ is a better quantity to compare than the CO luminosity $L_{\rm CO}$ because it depends on ν only through $T_b(J)$.

To derive the H_2 mass from the $L'_{\rm CO}$ involves some assumptions that have been adopted implicitly by all studies sofar. The first assumption is that the conversion ratio from $M(\rm H_2)$ to $L'_{\rm CO(1)}$ is the same as in the disk of the Milky Way galaxy: $\alpha = 4.6\ {\rm M_\odot\ (K\ km\,s^{-1}\ pc^2)^{-1}}$ (Solomon et al. 1987). The second assumption is that the $L'_{\rm CO}$ of the higher J transitions is comparable to $L'_{\rm CO(1)}$. Under these assumptions,

$$M(H_2) = \alpha L'_{\rm CO}. \quad (5)$$

Note that for ultra-luminous galaxies, the α factor is estimated to be three times smaller than the standard value for Milky Way (Solomon et al. 1997). α can be determined directly for each galaxy only when observations of different transitions at sufficient resolution become possible with interferometers operating at submillimeter wavelengths.

For the sources with no CO line detection to within the sensitivity limit, we adopt a 3-σ upper limit to the integrated CO intensity,

$$I_{\rm CO} \lesssim \frac{3\sigma_{rms}\Delta v}{\sqrt{N_{chan}}}\ {\rm K\,km\,s^{-1}}, \quad (6)$$

where $N_{\rm chan}$ is the number of resolution elements covered by Δv, and we have assumed a linewidth of $\Delta v = 300\ {\rm km\,s^{-1}}$.

Of the 23 galaxies we searched, we detected 2 confirmed CO sources from the galaxies: 0120+35 and 1440+26, both of which are luminous IR galaxies. Galaxy 0120+35 appears to be an interacting system with a tidal tail (Klaas & Elsässer 1993). We show the spectra of line emissions from CO$(1-0)$ and CO$(2-1)$ for galaxy 0120+35 in Fig. 1 and for galaxy 1440+26 in Fig. 2. Comparison of the CO(1-0) line temperatures measured at the 12m and the 30m telescopes suggests that the CO source is unresolved by the 30m beams. The ratio of the T_{mb} of the CO$(2-1)$ and the CO$(1-0)$ lines implies a (beam averaged) $T_b(2-1)\ /T_b(1-0)\ \approx (20/7) \times (13/24)^2 \approx 0.8$. This ratio is similar to that observed through optically thick clouds in the Galaxy and may imply that the molecular clouds of 0120+35 are quite closely packed within the 30m beam of $13''$ or 23 kpc at z = 0.11. The measured line ratios in 1440+26 are not so self-consistent, suggesting the CO emission may be more spatially extended compared to the $13''$ beam of the 30m telescope at the CO$(2-1)$ line.

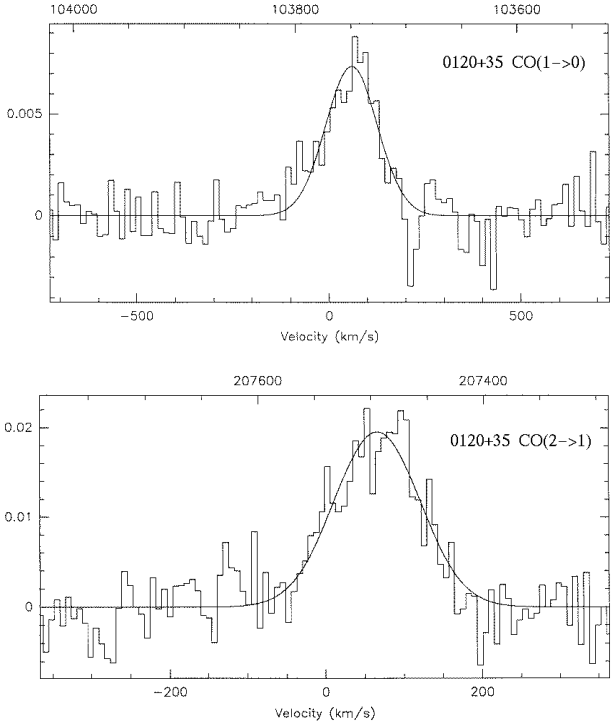

Fig. 1. The observed CO spectra of 0120+35 with IRAM 30m telescope, together with the best gaussion profile fit. The detail information is listed in Table 3.

The 12m marginal detection of CO(1-0) emission from 1630+84 could not be confirmed at the 30m. For 2011+83B, the 30m upper limit for the CO(1-0) line does not reach the marginal detection at the 12m, although the 30m upper limit for the CO(2-1) line is lower than the extrapolation from the 12m CO(1-0) result.

4. Discussion

We did not detect CO from any of the progenitors of luminous field galaxies in the redshift range of $0.35 < z < 1.06$, with upper limits to the H_2 mass of about $3 \times\ 10^{11}\ {\rm M_\odot}$. As some of the detected galaxies have H_2 mass up to $1.7 \times 10^{11}\ {\rm M_\odot}$ (cf. Table 1), these upper limits would suggest that intermediate z galaxies with H_2 mass much above $10^{11}\ {\rm M_\odot}$ are rare.

To examine the trend of the molecular gas content of galaxies at high z, we have combined our two confirmed detections for CO at $z \approx 0.1$ with other results in Fig. 3. In Fig. 3, we plot the observed quantity, L'_{CO} and the inferred H_2 mass of the

Table 2. MgII Absorption line systems observed in CO at IRAM 30 m

source	Coordinate $\alpha(1950)$	Coordinate $\delta(1950)$	z_a	z_e	CO line	T_{int} min	σ_{rms} mK	δv km s^{-1}	$M(H_2)$ $10^{10}M_\odot$
Q0109+200	01 09 28.90	20 04 24.00	0.5346	0.7460	(3→2)	486	0.8	26.6	< 4.2
					(2→1)	489	1.4	20.0	< 6.2
Q0229+131	02 29 01.94	13 09 45.00	0.4177	2.0670	(3→2)	82	5.6	24.6	< 17.8
					(2→1)	82	3.0	27.7	< 10.4
					(1→0)	30	6.1	46.1	< 27.4
Q0827+243	08 27 54.85	24 21 09.70	0.5248	0.9390	(3→2)	920	0.8	26.4	< 4.0
					(2→1)	920	1.0	29.7	< 5.2
Q0953+549	09 53 52.58	54 54 41.00	1.0590	2.5840	(4→3)	243	3.7	13.4	< 45.2
					(3→2)	143	6.0	26.8	< 103.4
					(2→1)	241	1.3	33.5	< 24.6
Q1019+309	10 19 39.32	30 56 21.90	0.3461	1.3190	(2→1)	143	9.7	26.3	< 22.9
					(1→0)	140	2.0	32.8	< 5.2
Q1622+239	16 22 32.43	23 52 02.00	0.6560	0.9270	(3→2)	708	1.5	21.5	< 10.2
					(2→1)	708	1.0	25.8	< 7.1
Q1821+107	18 21 41.69	10 42 44.40	0.4738	1.3640	(3→2)	116	2.7	25.6	< 10.9
					(2→1)	116	2.7	28.8	< 11.8
Q2128-123	21 28 53.20	-12 20 15.10	0.4299	0.5010	(3→2)	226	4.3	18.6	< 12.6
					(2→1)	226	2.9	27.9	< 10.6
					(1→0)	188	7.9	3.7	< 10.2

Table 3. Galaxies observed in CO (1→0) at NRAO 12 m

source	Coordinate $\alpha(1950)$	Coordinate $\delta(1950)$	z	$S_{100\mu m}$ Jy	T_{int} min.	σ_{rms} mK	δv_{bin} km s^{-1}	T_{peak} mK	Δv km s^{-1}	$M(H_2)$ $10^{10}M_\odot$
KE0038+34	00 38 22.6	34 31 29	0.1460	1.57	372	0.5	53.6	...	...	< 1.6
KE0120+35	01 20 52.9	35 25 17	0.1108	1.10	1020	0.3	52.0	1.3	148.2	1.0
KE0420+81	04 20 24.4	81 21 16	0.2400	< 1.10	636	0.4	58.1	...	...	< 2.9
KE0529+83	05 29 36.5	83 52 49	0.1743	1.2	276	0.6	30.6	...	...	< 1.9
KE0946+81[a]	09 46 23.6	81 41 32	0.1572	2.4	840	0.4	54.2	...	...	< 0.5
MK231[a]	12 54 04.7	57 08 39	0.0422	30.89	168	1.5	59.6	9.2	173.0	0.5
U02[a]	13 15 19.3	−15 32 54	0.5864	2.63	180	1.2	57.8	...	...	< 9.2
BR1321+05	13 21 48.5	05 52 40	0.1900	< 1.00	348	0.5	55.7	...	...	< 2.4
BR1403+44[a]	14 02 37.6	43 41 27	0.3200	1.28	384	0.6	61.8	...	...	< 1.7
1440+26 (U05)	14 40 33.0	26 34 15	0.1074	2.20	516	0.6	51.8	2.8	119.1	1.6
KE1630+84	16 29 31.4	84 06 33	0.1260	0.96	684	0.5	52.7	1.4	145.0	1.3
KE2011+83B	20 10 54.7	83 45 19	0.1272	1.31	1152	0.3	64.5	1.0	91.7	0.6
KE2011+83A	20 11 14.5	83 45 33	0.1253	...	180	0.7	52.7	...	...	< 1.7
U10	23 22 01.2	29 19 20	0.2401	< 1.00	288	0.6	58.1	...	...	< 4.3
AO0235+16	02 35 52.6	16 24 05	0.5243	...	312	0.6	71.4	...	...	< 13.5
Q0827+24	08 27 54.4	24 21 08	0.5247	...	840	0.5	71.4	...	...	< 11.3
G515E+A	15 22 00.3	08 19 40	0.0875	...	672	0.5	50.9	...	...	< 0.7
Q1821+10	18 21 41.7	10 42 44	0.4738	...	72	2.8	53.7	...	...	< 48.5

[a] Ultraluminous IR galaxies for which a factor of $1/3$ has been applied to α in computing the H_2 mass.

detected galaxies versus z. Besides the galaxies in our study (solid upper-limit symbols represent the observations from the 30 m telescope and the dotted upper-limit symbols represent the observations from the 12 m telescope), we also plot crosses to represent the 37 ultraluminous infrared galaxies (crosses) from Solomon et al. (1997), stars to represent the Cloverleaf H1413+117 (Barvainis et al. 1992), F10214+4724 (Solomon et al. 1992), BR1202−0725 (Omont et al. 1996), 3C48 (Scoville et al. 1993; Wink et al. 1997), 53W002 (Scoville et al. 1997), BRI1335−0417 (Guilloteau et al. 1997), and MG0414+0534 (Barvainis et al. 1998).

For the two lensed galaxies, the Cloverleaf and F10214+4724, the magnification factor (10 and 30, respectively; Yun et al. 1997, Eisenhardt et al. 1996) has been removed from the CO intensity measurements.

Table 4. IRAS galaxies observed in CO at IRAM 30 m

source	Coordinate $\alpha(2000)$	Coordinate $\delta(2000)$	z	CO line	T_{int} min.	σ_{rms} mK	δv_{bin} km s^{-1}	T_{peak} mK	Δv km s^{-1}	$M(H_2)$ $10^{10} M_\odot$
KE0120+35	01 23 43.4	35 40 55	0.1108	(1→0)	578	1.1	14.5	7.4	159.6	0.9
				(2→1)	140	3.1	7.2	19.6	128.8	0.4
1440+26(U05)	14 42 45.2	26 21 32	0.1070	(1→0)	334	1.7	14.4	5.8	219.3	0.9
				(2→1)	334	2.3	14.4	3.9	175.5	0.1
KE1630+84	16 22 17.2	83 59 53	0.1260	(1→0)	325	2.1	5.9	...	...	< 0.2
				(2→1)	350	5.2	7.3	...	...	< 0.2
KE2011+83B	20 04 44.4	83 54 09	0.1272	(1→0)	100	5.4	11.7	...	...	< 0.9
				(2→1)	145	9.3	5.9	...	...	< 0.2

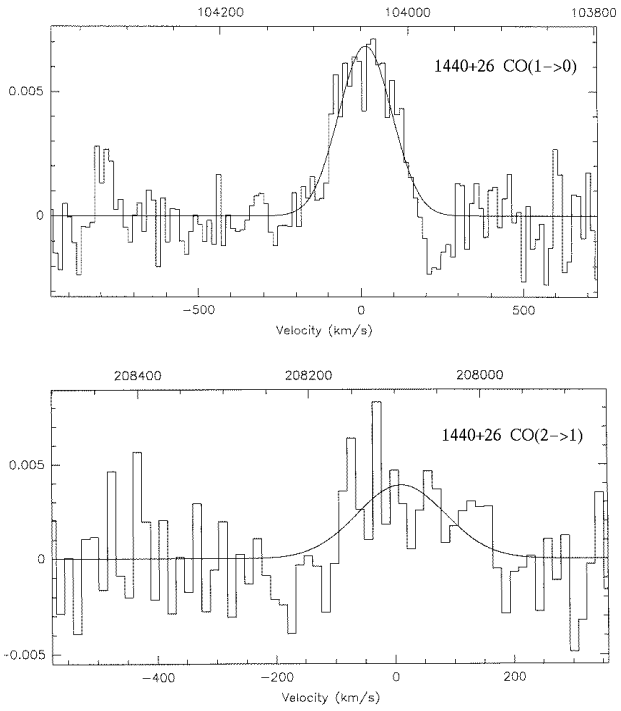

Fig. 2. The observed CO spectra of 1440+26 with IRAM 30m telescope, together with the best gaussion profile fit. The detail information is listed in Table 3.

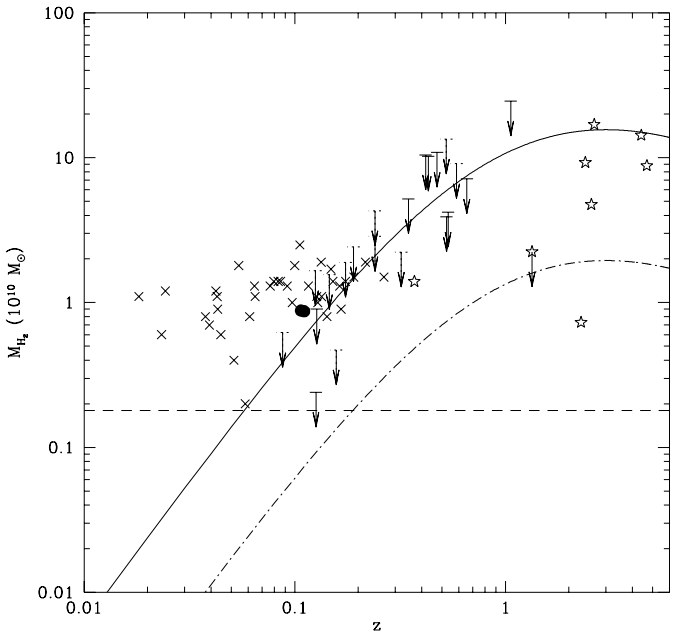

Fig. 3. The redshift distribution of the inferred H_2 mass from both our sample and the 37 ultraluminous infrared galaxies. Crosses are the ultraluminous infrared galaxies. Stars represent previous high-z detections and one non-detection, which are 3C48 at $z = 0.3695$, PG1634+706 at $z = 1.3371$, F10214+4724 at $z = 2.2855$, 53W002 at $z = 2.394$, H1413+117 at $z = 2.5585$, MG0414+0534 at $z = 2.639$, BRI1335−0417 at $z = 4.41$, and BR1202−0725 at $z = 4.69$. The dashed line represents the H_2 mass inside the Milky Way. The solid and dash-dotted curves represent the detection limits of the 30 m telescope at $I_{CO} = 0.8$ K km s^{-1} and $I_{CO} = 0.1$ K km s^{-1}. Note that the two lensed objects, F10214+4724 and H1413+117, have had the gravitational magnification factor removed, and that a smaller H_2-to-CO ratio has been adopted for 3C 48.

For the progenitors of luminous galaxies, we adopt $\alpha = 4.6\ M_\odot\ (\mathrm{K\ km\ s^{-1}\ pc^2})^{-1}$. For the ultraluminous galaxies, α is taken to be $1/3$ of the Galactic value, as suggested by Solomon et al. (1997). The H_2 mass of galaxies KE0946+81, U02, and BR1403+44 are computed according to the same smaller α as well, since all these three galaxies have an estimated far-IR luminosity $L_{\rm FIR} > 1 \times 10^{12} L_\odot$.

We also plot the detection limit of the 30m telescope (the solid curve) at $I_{CO} = 0.8$ K km s^{-1} and that corresponding to the limit at $I_{CO} = 0.1$ K km s^{-1} (the dash-dotted line), using the standard Milky Way $M(H_2)/L_{CO}$ ratio, $\alpha = 4.6\ M_\odot\ (\mathrm{K\ km\ s^{-1}\ pc^2})^{-1}$. The dashed line indicates the H_2 mass inside the Milky Way (Solomon & Rivolo 1989). We note that the upper limit to the H_2 mass for the galaxy, KE1630+84, approaches that of the Milky Way.

The observed upper limit to H_2 mass of $\sim 3 \times 10^{11}\ M_\odot$ in all the galaxies represented in Fig. 3 may be an indication that there exists some maximum baryon mass for condensation into individual galaxies.

To compare our IRAS faint galaxies with the 37 ultraluminous infrared galaxies from Solomon et al. (1997), we plot their velocity-integrated flux density of the CO$(1-0)$ line versus the infrared flux density in Fig. 4. Symbols are the same with

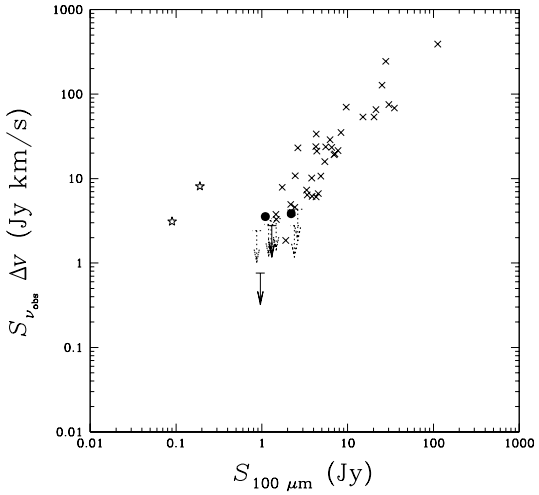

Fig. 4. The velocity-integrated flux density of the CO($1-0$) line versus the $100\mu m$ flux density. The stars represent the Cloverleaf quasar and BR1202-0725 with rest-frame 100 μm flux (Barvainis et al. 1995; Isaak et al. 1994).

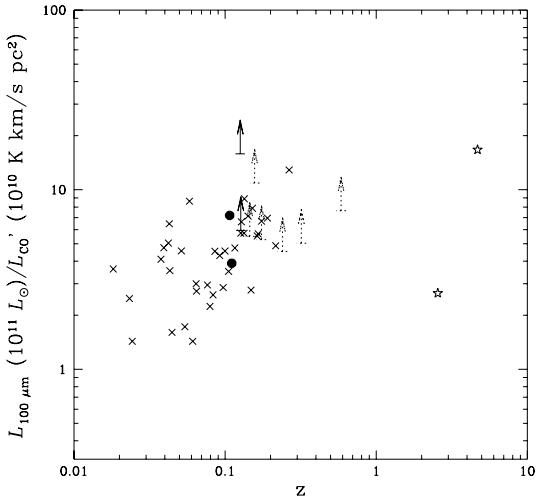

Fig. 5. Distance-independent quantity $L_{100\ \mu m}/L'_{\rm CO}$ versus redshift.

those in Fig. 3. The tight correlation between the CO($1-0$) flux and the 100 μm flux density from distant lumnious IR galaxies has been interpreted to indicate that the region of CO and IR emission is similar to a huge molecular cloud, i.e. a region of tightly packed dense molecular gas (Downes et al. 1993). As the two detections fit quite well with the essentially linear relation between the CO flux and the 100 μm flux density for the luminous galaxies, they have similar gas properties. The two distant quasars show deviations from the tight correlation, mainly because the detected CO line is from a higher J transition. In Fig. 5, there may be a slight rising trend of increasing $L_{100\mu m}/L'_{CO}$ with increasing z. This could be a selection effect since the detections for z > 2 galaxies are via high J transitions which would require excitation conditions that are more extreme than even in luminous IR galaxies.

5. Conclusions

Distant galaxies have become much more accessible to study in the optical and the near IR in the last few years, due to the Hubble Space Telescopes and large ground based optical telescopes and the rapid development of novel techniques, such as photometric redshifts. It is important to study in parallel the gas content of such galaxies. Our paper reports a modest first attempt to probe the gas content of intermediate redshift galaxies that may represent the majority of galaxies.

In our sample of progenitors to normal luminous field galaxies at $0.35 < z < 1.06$, H_2 gas content above $10^{11} M_\odot$ is rare. The same upper limit may apply to the luminous IR galaxies that are predominantly interacting galaxies, and distant quasars. Given that the H_2 mass of many gas rich galaxies is a substantial fraction of the dynamical mass (cf. Solomon et al. 1997), this upper limit to the H_2 mass, if universal, poses an interesting upper limit to the baryon content of protogalaxies. This should be compared to the upper limit to total galactic masses of $\sim 10^{12}\ M_\odot$, where the baryonic cooling time for gas of primordial composition exceeds the dynamical time (Blumenthal et al. 1984).

CO has been detected from the quasars BR1202-0725 at z=4.7 and BRI 1335-0417 at z=4.4, so that at least in these two quasars, the ISM in the host galaxy has been enriched by the time the Universe is less than 1 Gyr old (Omont et al 1996). Furthermore, the 1.3 mm continuum implies that $\sim 10^8\ M_\odot$ of dust have already been formed. An extensive survey for such galaxies at high z would have very significant implications for and provide a different approach to deciphering the star formation history in the early universe.

A thorough investigation of gas content in distant galaxies has to await a substantial increase in sensitivity and resolution. In "normal" galaxies in which the ISM is relatively quiescent and similar to the Milky Way, the CO($1-0$) transition is stronger than the higher transitions. So, future studies of high z "normal" galaxies should be conducted in the CO($1-0$) line in the 115/(1+z) GHz range.

Acknowledgements. This project was started during KYL's sabbatical in 1994 at the Institute of Astronomy and Astrophysics as a National Science Council Guest Professor, and continued at the Max-Planck-Institut für Extraterrestrische physik under an Alexander von Humboldt Research Award. KYL also thanks the Research Board of the University of Illinois for financial support for HWC and some of the observing trips. We thank Dr. C. Steidel for providing his sample of progenitors of luminous field galaxies obtained from his search for the absorbers causing the MgII absorption in QSO spectra, Drs. Jun-Hui Zhao and Shudong Zhou for communications about the study of ultra-luminous IR galaxies before publication, S. Y. Liu for help in preparing an initial version of the manuscript and the staff of IRAM for their expert assistance at the 30m.

References

Barvainis R., Antonucci R., Coleman P. 1992, ApJ 399, L19
Barvainis R., Tacconi L., Antonucci R., Alloin D., Coleman P. 1994, Nat 371, 586

Barvainis R., Antonucci R., Hurt T., Coleman P., Reuter H.-P., 1995, ApJ 451, L9
Barvainis R., Alloin D., Guilloteau S., Antonucci R., 1998, ApJ 492, L13
Blumenthal G., Faber S., Primack J., Rees M., 1984, Nat 311, 517
Brown R.L., Van den Bout P.A., 1992, ApJ 397, L19
Downes D., Solomon P.M., Radford S.J.E., 1993, ApJ 414, L13
Eisenhardt P.R., Armus L., Hogg D.W., et al., 1996, ApJ 461, 72
Ellis R.S., 1997, AR&A 35, 389
Guilloteau S., Omont A., McMahon R.G., et al. 1997, A&A 328, L1
Guzmán R., Gallego J., Koo D.C., et al., 1997, ApJ 489, 559
Isaak K.G., McMahon R.G., Ellis R.E., Withington S., 1994, MNRAS 269, L28
Klaas U., Elsässer H., 1993, A&AS 99, 71
Lanzetta K.M., Yahil A., Fernandez-Soto A., 1996, Nat 381, 759
Ohta K., Yamada T., Nakanishi K., et al., 1996, Nat 382, 426
Omont A., Petitjean P., Guilloteau S., et al., 1996, Nat 382, 428
Scoville N.Z., Padin S., Sanders D.B., et al., 1993, ApJ 415, L75
Scoville N.Z., Yun M.S., Windhorst R.A., et al., 1997, ApJL 485, L21
Solomon P.M., Rivolo A.R., Barrett J.W., Yahil A., 1987, ApJ 319, 730
Solomon P.M., Rivolo A.R., 1989, ApJ 339, 919
Solomon P.M., Downes D., Radford S.J.E., 1992, ApJ 398, L29
Solomom P.M., Downes D., Radford S.J.E., Barrett J.W., 1997, ApJ 478, 144
Steidel C.C., 1993, In: Shull J.M., Thronson H.A. (eds.) The Environment and Evolution of Galaxies. Kluwer, Dordrecht, p. 263
Steidel C., Giavalisco M., Pettini M., Dickinson M., Adelberger K., 1996, ApJ 462, L17
Steidel C., Adelberger K., Dickinson M., et al., 1998, ApJ 492, 428
Wiklind T., Combes F., 1994, A&AL 288, 41
Wink J.E., Guilloteau S., Wilson T.L., 1997, A&A 322, 427
Wolfe A.M., Turnshek D.A., Smith H.E., Cohen R.S., 1986, ApJS 61, 249
Wolfe A.M., Prochaska J.X., 1998, ApJ 494, L15
Yun M.S., Scoville N.Z., Carrasco J.J., Blandford R.D., 1997, ApJ 479, L9